POLITECNICO DI TORINO
Repository ISTITUZIONALE

Nonlinear dynamic analysis of gas turbine combustor leaf seal

(Article begins on next page)

16 July 2022

Nonlinear dynamic analysis of gas turbine combustor leaf seal

L. R. Tamatam [1], **D. Botto** [1], **S. Zucca** [1], **F. Funghi** [2]
[1] Department of Mechanical and Aerospace Engineering,
Politecnico di Torino, Corso Duca degli Abruzzi 24, 10129, Torino, Italy
e-mail: **lakshminarayana.tamatam@polito.it**

[2] Baker Hughes (Nuovo Pignone s.r.l.),
Florence, Italy

Abstract

The leaf seals are one of the typical sealing systems in gas turbine and jet engines. In Baker Hughes LT family gas turbines, they are used to create sealing between the combustion chamber and the first stage nozzle. The leaf seals are thin metallic plates and subjected to dynamic loads and high temperatures. They have curved contacts, and depending on the inclination, they can experience partial contact. Furthermore, when excited by dynamic loads, the leaf seal can be subject to intermittent contact, possibly triggering wear out or vibratory phenomena. Due to its flexibility and its partial seating, it exhibits a complex nonlinear dynamic behaviour, strongly variable with the operating conditions. This study presents a numerical investigation using coupled static/dynamic harmonic balance method (HBM) frequency-based solution technique. The reported solutions include nonlinear forced response and contact studies for various operating and kinematic conditions along with brief insights.

1   Introduction

Gas turbine engines are widely used in aviation to propel aircraft, electric power generation, pumping natural gas through pipelines, oil refining process and other applications given their very high power to weight ratio, small size and efficiency. Hence, these powerhouses are designed to perform at its structural limits to maximise the output and increase the efficiency and of course, to have high reliability. In the present study, one such component of the engine is analysed for its complex dynamic behaviour and reliability.

Leaf seals are located in the annulus of the combustor section of a Gas Turbine Engine (GTE). Two sets of inner and outer leaf seals provide sealing and prevent the leakage of the combustion mixture from the combustor section to the surroundings. The leaf seals have two curved contact patches, as shown in Figure 1 – between the nozzle and leaf seal, and the liner and the leaf seal. Given the location between the end of the combustor section and high-pressure turbine section, they experience high dynamic forces and acoustic pulsation. These seals work at high operating temperatures. They are designed to withstand a range of operating and kinematic envelopes and provide the sealing. Due to the curved contact nature, the two contacts on the leaf seal experience partial contact either at the edges or at the centre given the positive or negative inclination of the leaf seal and the dynamic behaviour. The leaf seal is mounted to the nozzle via two pins and two spiral springs surrounding the pins to allow sufficient play during the operation. However, the leaf seal may look simplistic in geometry, but their complex dynamic behaviour is primarily governed by the contact conditions and dynamic excitation. From the field tests, it is found the leaf seal experience dominant wear at the contact zones. The wear is caused due to partial intermittent contact at the contact zones. The wear pattern is also random sometimes concentrated at the centre or the edges of the contact patch, meaning the leaf seal experiences different intermittent contact behaviour for different operating

conditions. Hence, it is of high importance to investigate the complex nonlinear dynamic behaviour of the leaf seal when subject to various operating and kinematic envelopes.
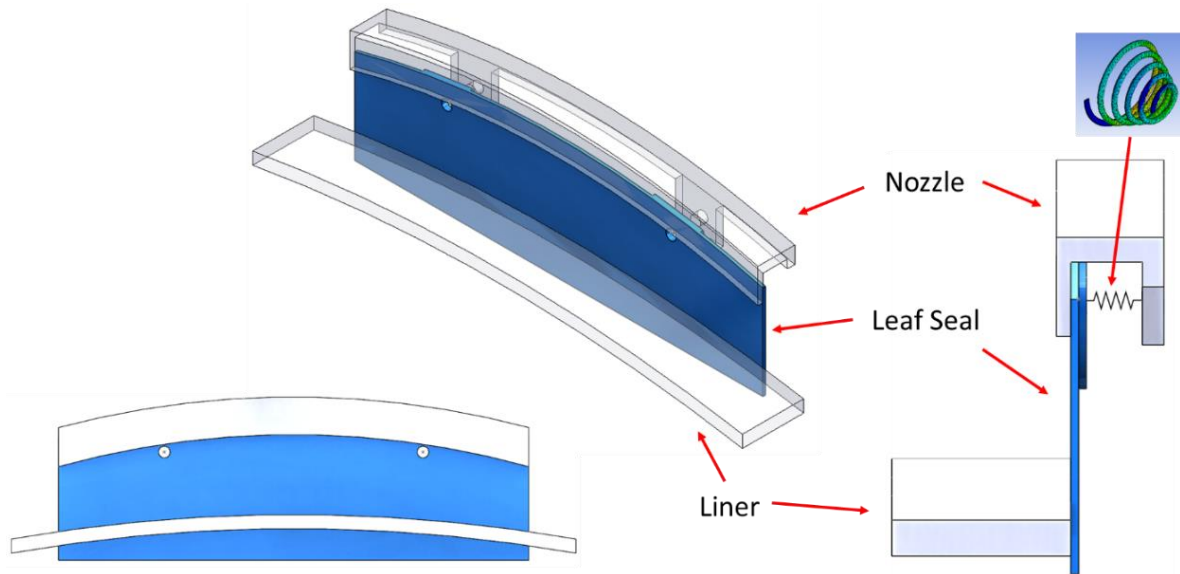

Figure 1: Combustor Leaf Seal

The current study is a numerical work to investigate the nonlinear dynamic behaviour of leaf seal experiencing intermittent contact using a proven static/dynamic coupled approach with multi-harmonic balance method (HBM) ([1], [2]). Concerning the previous works existing in the literature ([3], [4]), the current approach allows the automatic update of the static pre-load distribution over the contact area during the nonlinear dynamic analysis, without any need for a separate static analysis. This is particularly helpful to model the intermittent contact behaviour where the static analysis is highly dependent on the contact condition. The current study presents linear analysis, nonlinear forced response and contact behaviour for various operating and kinematic envelopes along with the sensitivity study of other parameters.

2   Methodology

The contact interface introduces non-linearity to the system of equations. Two ways to solve the nonlinear differential equation is using time domain and frequency domain methods. A time-domain method such as Direct Time Integration (DTI) provides the transient as well as steady-state response but is computationally very demanding and is not a feasible solution for practical scenarios and large systems. The state-of-the-art frequency-domain method to compute the nonlinear response is the Harmonic Balance Method (HBM). This method assumes a periodic response under periodic excitation. Krack and Gross's book [5] provides a detailed description of the method and examples of nonlinear vibration problems. This method offers speedy solution times assuming steady-state response and much less computationally demanding relative to the time domain methods. In our case, this is better as we are looking only for the steady-state response of the system.

The current study uses a more recent formulation of the HBM, which allows performing a coupled static and dynamic analysis of the system. This coupled method is proven to provide better results in terms of accuracy with respect to classical uncoupled approaches [3]. It is comparable to the accuracy of direct time integration results with sufficient harmonics.

2.1   Governing equations

The governing equation of motion of a system with contact interfaces undergoing periodic vibrations is written as:

$$\mathbf{m}\ddot{\mathbf{q}}(t) + \mathbf{c}\dot{\mathbf{q}}(t) + \mathbf{k}\mathbf{q}(t) = \mathbf{f}(t) + \mathbf{f}_c(\mathbf{q}, \dot{\mathbf{q}}, t) \tag{1}$$

where $\mathbf{m}$, $\mathbf{c}$ and $\mathbf{k}$ are the mass, viscous damping and stiffness matrices, $\mathbf{q}(t)$ is a displacement vector; $\mathbf{f}(t)$ is the excitation force vector; $\mathbf{f}_c(\mathbf{q}, \dot{\mathbf{q}}, t)$ are nonlinear contact force vectors. To solve the equation (1) for periodic excitation using HBM, the periodic quantities with an angular frequency of ω are expressed as truncated series of harmonic terms:

$$\mathbf{q}(t) = \sum_{h=0}^{H} \widehat{\mathbf{q}}^{(h)} e^{ih\omega t} \; ; \; \mathbf{f}(t) = \sum_{h=0}^{H} \widehat{\mathbf{f}}^{(h)} e^{ih\omega t} \; ; \; \mathbf{f}_c(\mathbf{q}, \dot{\mathbf{q}}, t) = \sum_{h=0}^{H} \widehat{\mathbf{f}}_c^{(h)}(\widehat{\mathbf{q}}) e^{ih\omega t} \tag{2}$$

The time-domain nonlinear differential equation (1) is transformed into a nonlinear algebraic equation using Galerkin projection with Fourier coefficients as defined in equation (2) and written as:

$$\mathbf{D}^{(h)}\widehat{\mathbf{q}}^{(h)} = \widehat{\mathbf{f}}^{(h)} + \widehat{\mathbf{f}}_c^{(h)}(\widehat{\mathbf{q}}) \; with \; h = 0..H \tag{3}$$

where $\mathbf{D}^{(h)} = (\mathbf{k}^{(h)} - h^2\omega^2\mathbf{m}^{(h)} + ih\omega\mathbf{c}^{(h)})$. The equation (3) consists of the static ($h = 0$) and dynamic ($h = 1..H$) equations of the system coupled to each other by Fourier coefficients of the nonlinear contact force $\widehat{\mathbf{f}}_c$ depending on the Fourier coefficients of the displacement $\widehat{\mathbf{q}}$. The number of harmonics H is determined by the accuracy of the results needed.

The residual equation is given by:

$$\mathbf{RES}^{(h)} = \mathbf{D}^{(h)}\widehat{\mathbf{q}}^{(h)} - \widehat{\mathbf{f}}^{(h)} - \widehat{\mathbf{f}}_c^{(h)}(\widehat{\mathbf{q}}) \; with \; h = 0..H \tag{4}$$

As the nonlinear solvers to be used to solve the above equation accepts only real values, the complex form residual equation is split into its real and imaginary components to minimize the residual to an acceptable tolerance as:

$$\mathbf{RES} = \left[\mathbf{RES}^{(0)}, \mathfrak{R}(\mathbf{RES}^{(1)}), \mathfrak{I}(\mathbf{RES}^{(1)}) \dots \mathfrak{R}(\mathbf{RES}^{(H)}), \mathfrak{I}(\mathbf{RES}^{(H)})\right]^{\mathrm{T}} \tag{5}$$

2.2   Contact Model

A contact model is necessary to compute the nonlinear contact forces mentioned in the previous section. There are various node-to-node and patch-to-patch contact models available in the literature ([6]–[15]) such as Coulomb slider, Jenkins element – 2D and 3D with constant and variable normal load, Iwan model and its variations, Bouc-Wen model, Valanis model, LuGre model etc. In our study, we chose the state-of-the-art node-to-node 2D Jenkins element with a variable normal load to compute the contact forces, as shown in Figure 2(a). A typical hysteresis loop generated for the given input force and displacements is shown in Figure 2(b). The solution of equation (3) requires the contact forces $\widehat{\mathbf{f}}_c$ on the contact interface as input. The contact element is characterized by two linear springs in the tangential and normal direction with tangential (k_t) and normal (k_n) contact stiffness, at each node pair over the contact interface. The contact model allows to characterize and simulate three possible contact states – stick, slip and lift-off. Due to space constraints, the contact model and the governing equations are not mentioned here in detail. Refer [4] for a detailed working principle.

The governing equation (3) is solved in the frequency domain using HBM, whereas the accurate contact forces are possible to compute only in the time domain. Hence an Alternate Frequency/Time (AFT) method ([16], [17]) is employed. The relative displacements are converted from the frequency domain to the time domain by applying Inverse Fast Fourier Transform and then run through the contact model. The contact forces are obtained in the time domain. Then applying Fast Fourier Transform to the contact forces to convert to the Fourier coefficients, as shown in Figure 3.
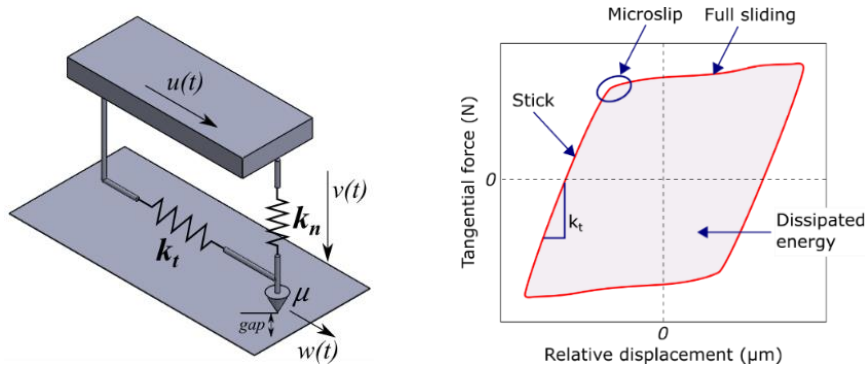
Figure 2: (a) Jenkin's element contact model with variable normal load, (b) A typical hysteresis loop
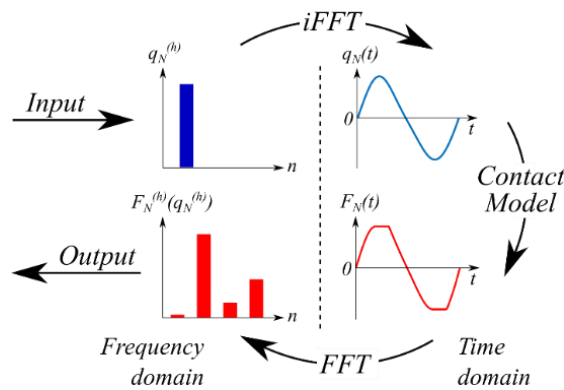

Figure 3: Alternating Frequency Time (AFT) method

Trust-region based algorithm is implemented for the iterative procedure in MATLAB to solve the nonlinear equations. The Jacobian matrix needed to solve the set of nonlinear equations is computationally intensive if using MATLAB built-in finite difference method (FDM) for large systems. Hence an analytical Jacobian is implemented based on the works of [18], [19]. This dramatically increases the speed of the solution by many folds. The contact forces and computation of the dynamic response are primarily based on the accurate input of the normal and tangential contact stiffness. The closed-form solutions needed to compute the accurate tangential (k_t) and normal (k_n) contact stiffness to provide the contact model is provided based on the analytical equations as mentioned in Ref [20]–[23]. The contact stiffnesses of elastic bodies can also be computed using numerical method as shown in Ref [24]. Then, the resulting contact stiffnesses are distributed over the contact area according to the individual elemental contribution.

3 Results

3.1 Leaf Seal system description

Figure 4 shows the schematic of the leaf seal system along with the boundary conditions. The leaf is held on to the nozzle via two pins and two encasing spiral springs. The front leg of the nozzle acts as a stopper for the leaf with the compression of the springs and makes contact between the leaf and the nozzle. On the bottom half of the leaf, there is a liner which mates the leaf seal and making it a lower contact patch. Hence, there are two curved contact patches. The liner can be stationary or have an independent harmonic displacement. For the dynamic analysis, modelling of the nozzle and the liner can be omitted as they act as a fixed ground at the nozzle and moving ground at the liner contact. The right-side figure shows the simplified schematic with the necessary boundary conditions to model the system for dynamic analysis. The contact is assumed by equivalent springs with normal contact stiffness. The dynamic excitation is applied on one side and static pressure on the other side of the leaf as shown.
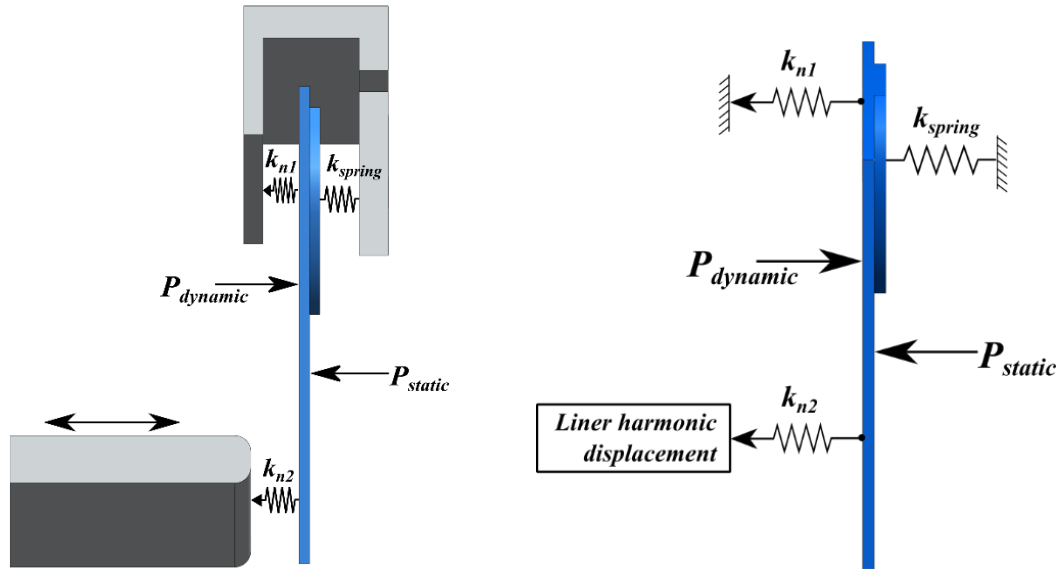
Figure 4: Schematic of the Leaf Seal and the boundary conditions – side view (left),Simplified schematic used for the dynamic analysis (right)

Figure 5 shows the 3D FE mesh of the leaf seal. The FE mesh is generated using ANSYS. The upper and lower contact patch is highlighted in green colour. Each contact patch is discretized using three rows of 21 node-to-node contact elements as described in the previous section. In total, 126 contact elements for the leaf seal. This is a sufficient number of contact elements to track the dynamics accurately and to see the change in the contact conditions for various scenarios.
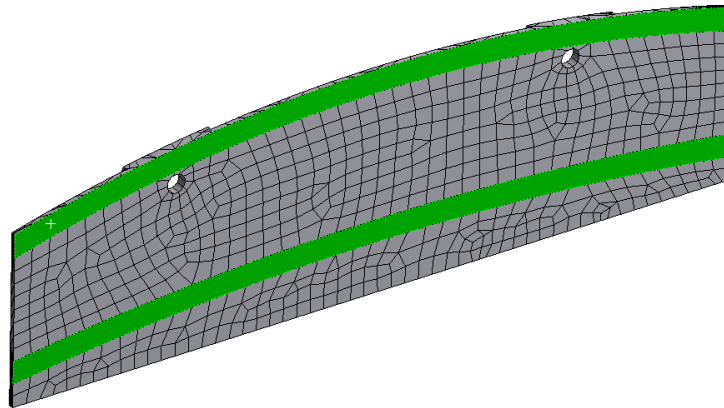

Figure 5: 3D FE Mesh of the Leaf Seal with highlighted upper and lower contact patches (in green)

The material properties of standard Steel at room temperature are considered. Though the operating temperature is higher, it is omitted for this study. Also, the dimensions of the leaf seal are academic version. They do not correspond to the actual dimensions out in service in a typical GTE. As the intermittent contact is modelled in normal direction alone, any slip in radial direction and friction is omitted. The contact is modelled using a unilateral contact in the normal direction with an assumed normal contact stiffness. As mentioned in the methodology, considering the full size of the leaf seal with all DOFs for dynamic analysis is prohibitively expensive with computation burden and is unnecessary. Hence, a Craig-Bampton Component Mode Synthesis Reduced Order Modelling (CB-CMS ROM) is performed retaining the contact nodes, excitation and response nodes as master nodes, the rest as slave nodes. With 142 contact nodes giving 284 DOFs and 20 retained modes, the size of the dynamic system is 304 DOFs. One harmonic is considered along with the 0th harmonic for the solution procedure. Figure 6 shows the range of kinematic envelope seen in actual operating conditions.
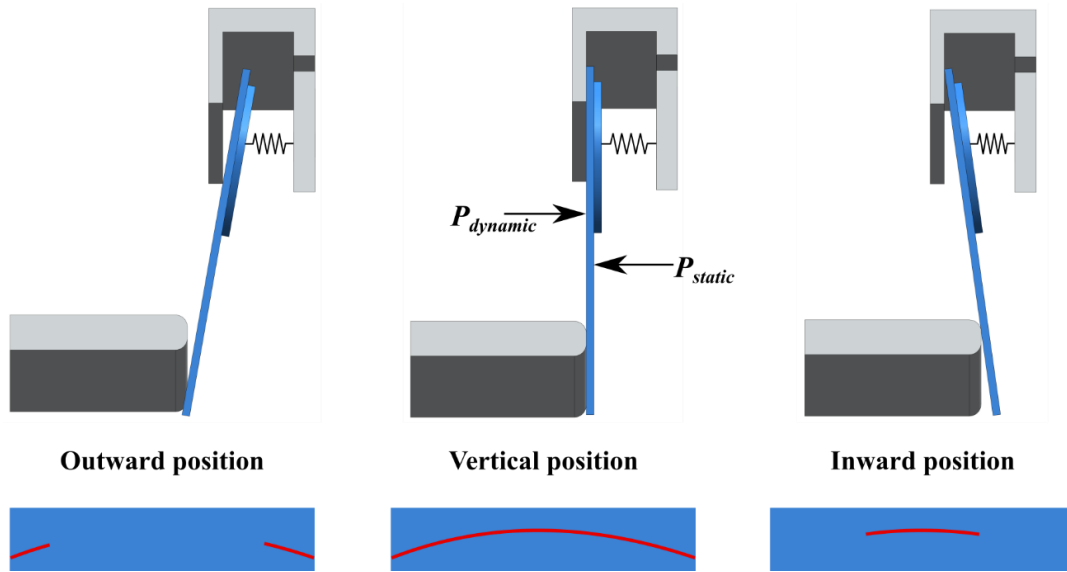
3.2   Kinematic and operating envelope

Figure 6: Kinematic envelope showing the inward and outward leaf seal inclination driven by the liner displacement. [Note the partial contact area (edges or centre) when the leaf seal is not in vertical position due to the nature of curved contact]

A parametrised sensitivity analysis is performed to study the effect of various encompassed operating and kinematic envelope. This would help to study the effect of the individual parameter has on the dynamics of the leaf seal and the contact status conditions. The parameters considered for the analysis are:

1. Effect of Liner displacement (see Table 1)
2. Effect of excitation force
3. Effect of liner displacement only – without excitation force
4. Effect of normal contact stiffness (K_n)
5. Effect of pin spring stiffness (K_{spring})

Table 1: Tabular representation of various normalized liner displacement conditions

Condition #	Normalized liner displacement	
	Static (0th harmonic)	Harmonic (1st harmonic)
1	0	0
2	1	0
3	-1	0
4	0	1
5	0	$1i$
6	1	1
7	-1	1

3.3   Interpretation of the scheme of results presented using sample plots

Figure 7 shows two response curves corresponding to the 'linear free' and 'linear stick' case for the two configurations shown in the boxes, respectively. The nonlinear response is then overlapped on these linear base curves, which aids to compare the response and to see whether the behaviour is closer to the free or stick case.
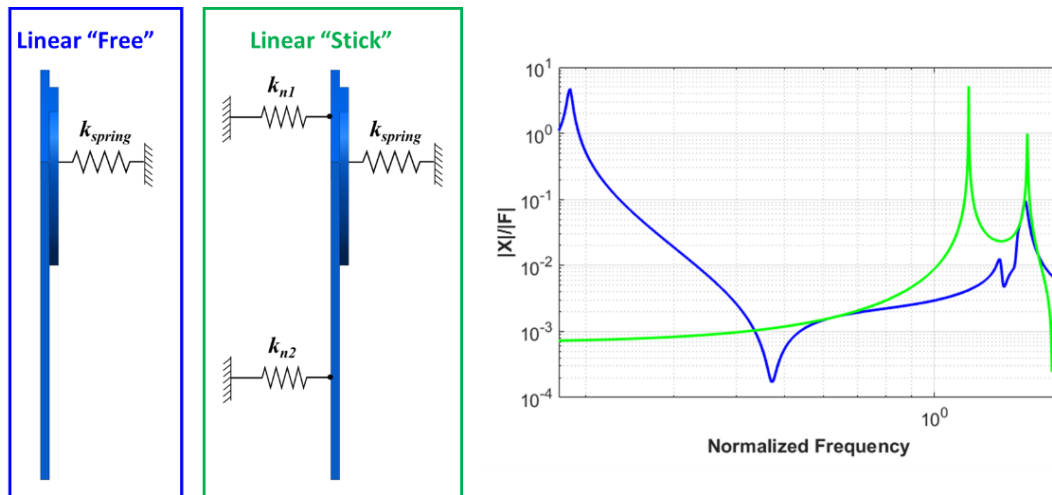
Figure 7: Sample response curve showing "linear free" and "linear stick" cases corresponding to an arbitrary node DOF in order to compare the nonlinear response

Figure 8 shows the response plots corresponding to the three nodes of the leaf as highlighted – top figure at the centre node of the upper contact patch, the middle figure at the geometric centre of the leaf seal and the bottom figure corresponding to the bottom corner of the leaf seal. This is in the hope to capture most of the dynamics with the help of these three graphs (as minimum as possible). Ideally, there exists data to plot similar graphs for all the master nodes selected.

The response has two linear free and linear stick cases in blue and green coloured lines, respectively. The red coloured line is the nonlinear dynamic response of the system for a set of boundary conditions.
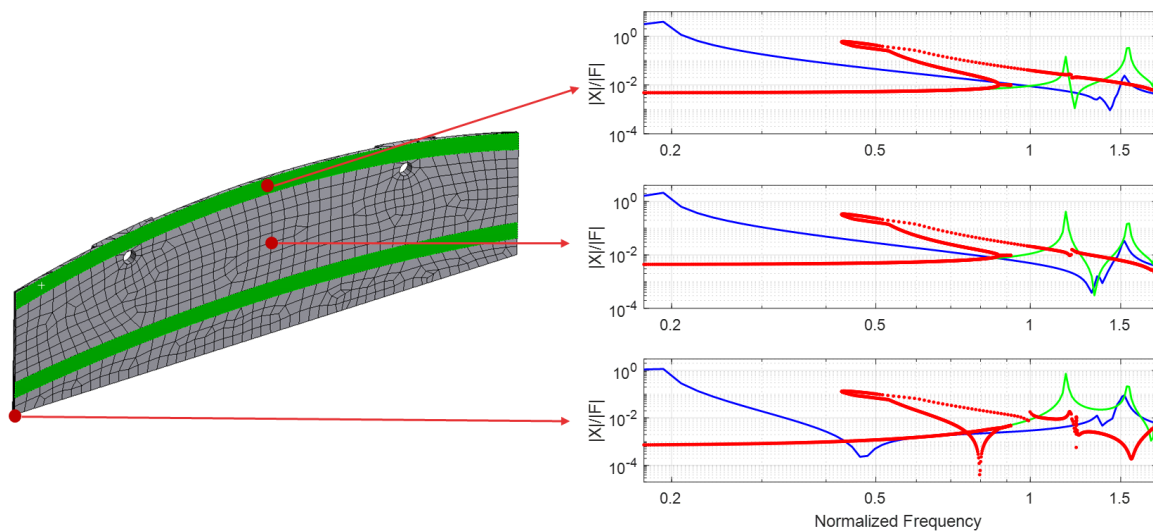

Figure 8: Sample response curves pattern showing the corresponding nodes of the leaf seal to follow the pattern in the results section

The above plots show the response amplitude versus frequency for a range of frequencies. However, it does not provide any information on the contact status, contact pressure, etc. Hence, Figure 9 provides the complementing information for a choice of frequency from the response plots. In this figure, the two contact pressure plots are shown corresponding to the upper and lower contact patch. Similarly, the contact status plots for the upper and lower contact patch are shown indicating whether the contact status at each contact node is in stick, separation-stick or full separation during one vibration cycle at that particular frequency. The contact patch is discretized with three rows of 21 contact elements, which is 63 contact elements for each patch.
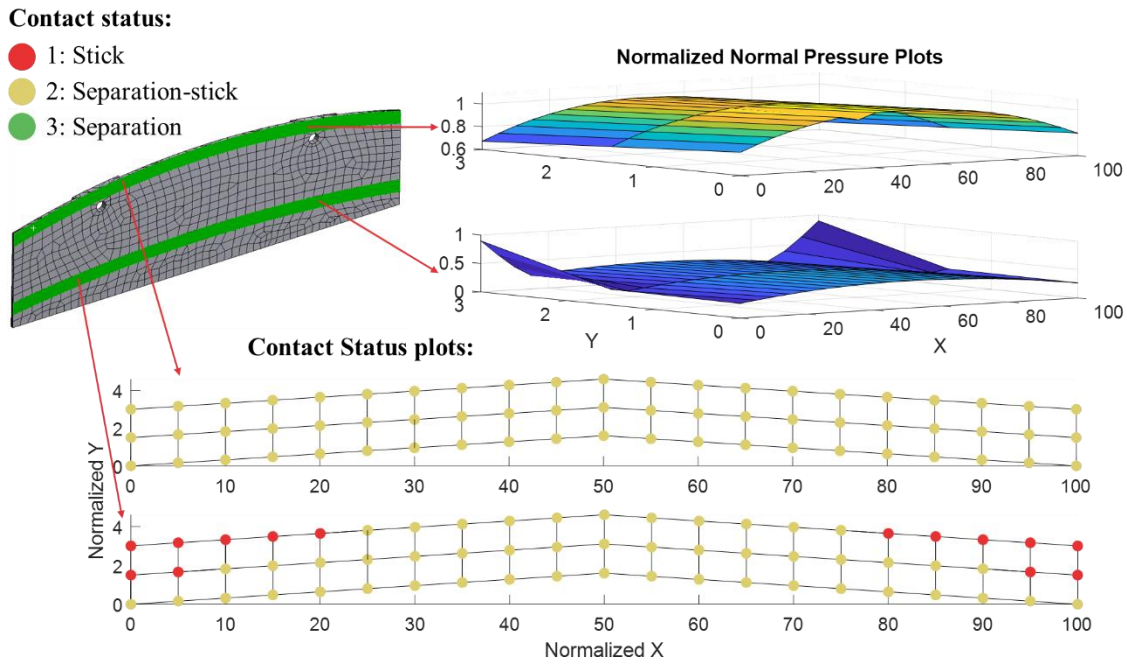
Figure 9: Sample contact pressure plots and contact status plots corresponding to the upper and lower contact patches to follow the pattern in the results section

3.4   Modal analysis and forced excitation results

Figure 10 shows the different configurations of leaf seal with just the leaf, free, and stick conditions at the contact patches. Table 2 lists the natural frequencies of the first 10 modes for the given three conditions. In just the leaf seal configuration, there are two rigid body modes for the given kinematic envelope after imposing the displacement constraints. By imposing the two springs at the pin and spring configuration, we arrive at the second configuration. Now the rigid body modes are eliminated, but the natural frequencies are very low because the imposed springs are very soft in nature. In the first two modes, the dynamics are entirely governed by the springs, and the leaf acts as a rigid body. Of course, in the third configuration, where the contact is fully constrained by the imposed linear springs with normal contact stiffness (K_n), the resonant frequencies are higher as the system is stiffer.
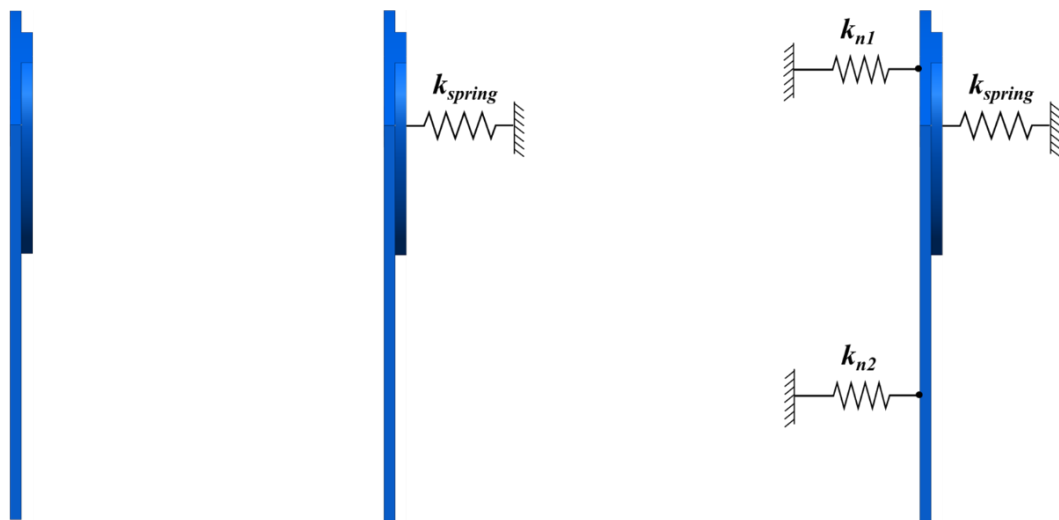

Figure 10: (a) Leaf Seal (free condition), (b) Leaf Seal with springs (free condition),(c) Leaf Seal with springs and grounded contacts (stick condition)

Table 2: Linear Modal analysis of the Flat Leaf Seal with free and fully stuck contact configurations

Leaf Seal – Free condition		Leaf Seal with springs – Free condition		Leaf Seal – Fully Stuck condition	
Mode #	Normalized Frequency	Mode #	Normalized Frequency	Mode #	Normalized Frequency
1	0.00	1	0.01	1	1.17
2	0.00	2	0.19	2	1.54
3	1.00	3	1.35	3	1.59
4	1.71	4	1.53	4	2.29
5	2.44	5	2.43	5	2.73
6	3.96	6	3.96	6	4.15
7	4.78	7	4.78	7	4.95
8	5.73	8	5.73	8	5.81
9	6.00	9	6.00	9	6.11
10	7.11	10	7.11	10	7.24

3.4.1 Forced response results

This section presents the complex nonlinear dynamic response plots for a vertical leaf seal with static liner configuration. Due to space constraints, only one set of results is shown. The normalized stiffnesses of mounting spring stiffness (K_{spring}) and the normal contact stiffness (K_n) is assumed to be 1 and 25, respectively.
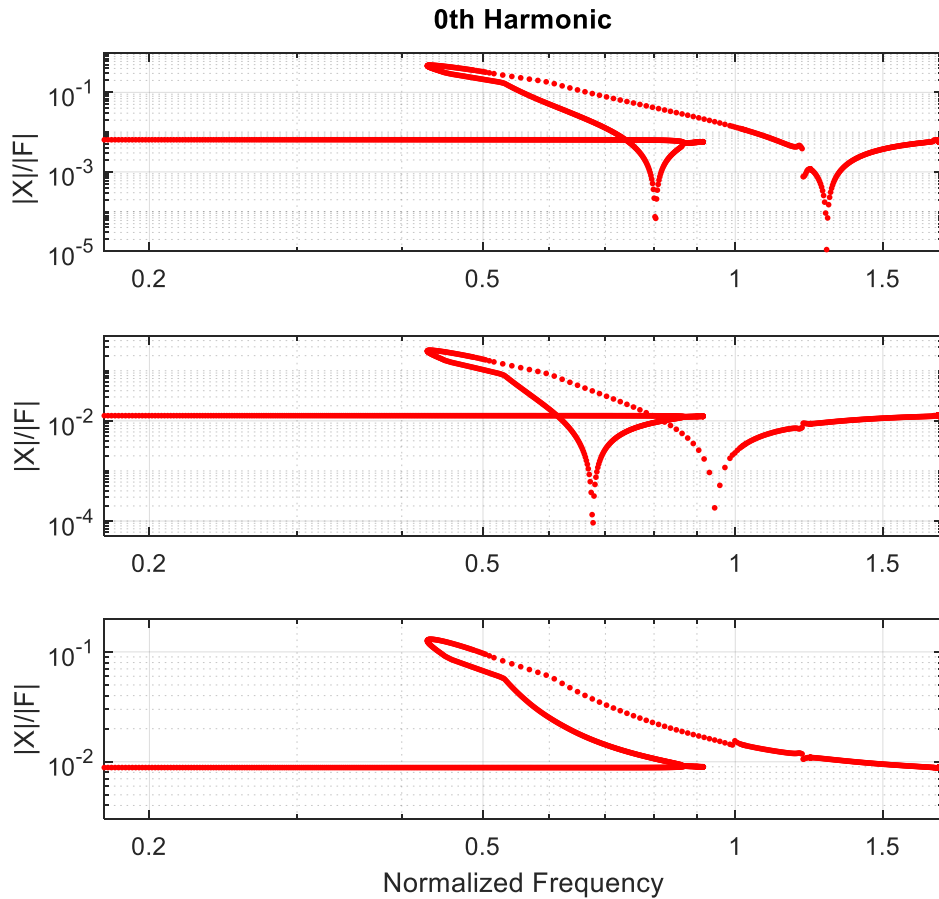

Figure 11a: Nonlinear response for the vertical leaf seal with static liner configuration (0th harmonic)
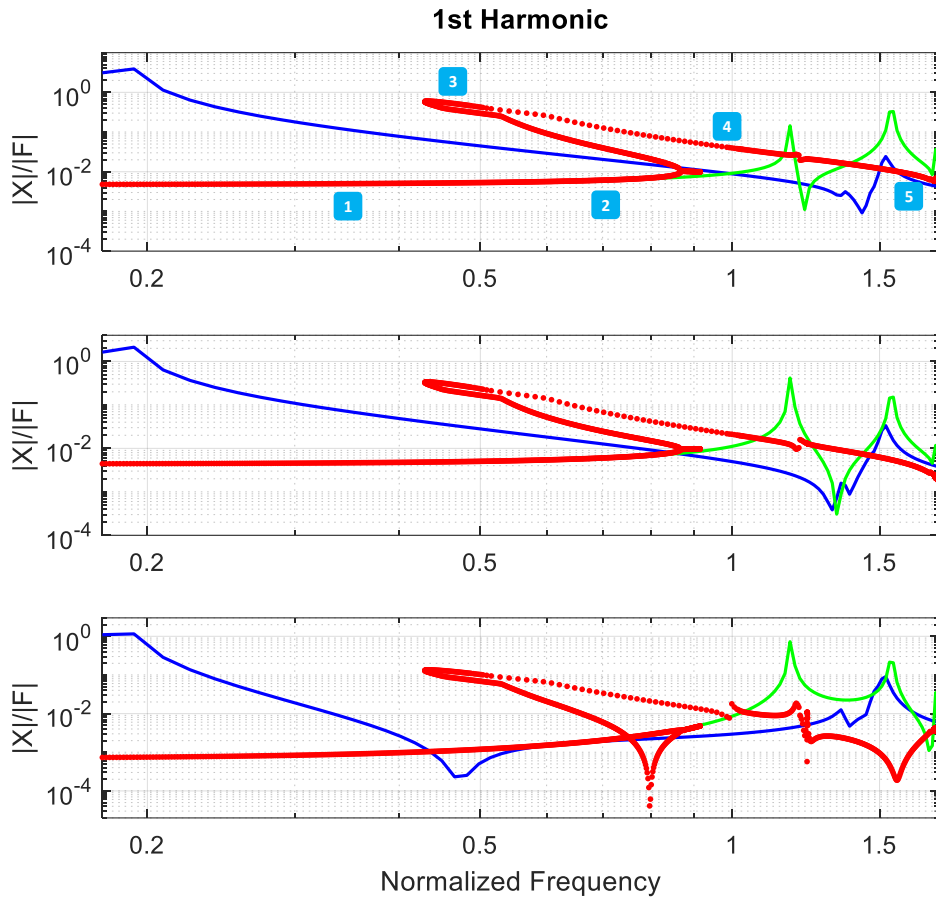
1st Harmonic

Figure 11b: Nonlinear response for the vertical leaf seal with static liner configuration (1st harmonic) (blue – linear free state, green – linear stick state, red – nonlinear response)

The dynamic response (red line) can be classified into a linear regime and nonlinear regime. The nonlinear regime corresponds to the frequency range where the 'jump phenomena' ([10], [25]) or the softening behaviour is exhibited and deviates from the linear response. The rest is the linear regime.

Generalizing for various cases performed on the sensitivity study, the leaf seal system exhibits softening behaviour non-linearity due to intermittent contact behaviour at the two contact patches. This softening behaviour tends to have multiple solutions at a given frequency as seen in the figure in the nonlinear frequency range. The peak response amplitudes are dominantly higher in the resonance zone and can be destructive if the system continued to operate in this range for a longer period. The partial or full loss of contact on the leaf seal in one vibration period, leads to impact behaviour and loss of material, thereby creating wear phenomena. For reference, an experimental investigation of fretting wear behaviour at high temperatures provides insights on the relationship of contact loads and wear properties [26]. The length of the 'softening branch' and peak amplitude for each case is dependent on the placement and excitation of the liner.

3.4.2   Contact status insights corresponding to forced response plots

The below contact status and contact pressure plots corresponding to the frequencies in response plot Figure 11 indicate the general trend of contact behaviour such as fully stuck region, partial separation-stick region and/or full separation region. The frequencies corresponding to the linear regime, i.e., in plots numbered '1' and '5', the contact nodes at the curved contact patches are fully stuck. In other words, when the leaf seal is subject to operation in these frequencies, the contact between the leaf seal and nozzle, and between liner and leaf seal are fully adherent. So, there is no separation, and likely no wear occurs. However, in the

nonlinear regime exhibiting jump phenomenon, in plots numbered '2', '3' and '4' partial contact elements exhibit separation behaviour. The vibration amplitudes are also higher. With the partial separation in one vibration cycle, leads to chattering, hence, creating wear. This wear can be amplified with increase in operation cycles. Also, the partial separation behaviour could trigger and enhance the complex nonlinear behaviour creating a snowball effect, hence leading to higher vibration amplitudes and branch switching. Especially in the plots numbered '3' and '4', where almost all the contact elements experience separation stick behaviour in a given vibration period. This is detrimental to the designed service life and maximum vibration amplitudes. Hence it is vital to mitigate and control the high amplitude and jump phenomena behaviour beforehand.
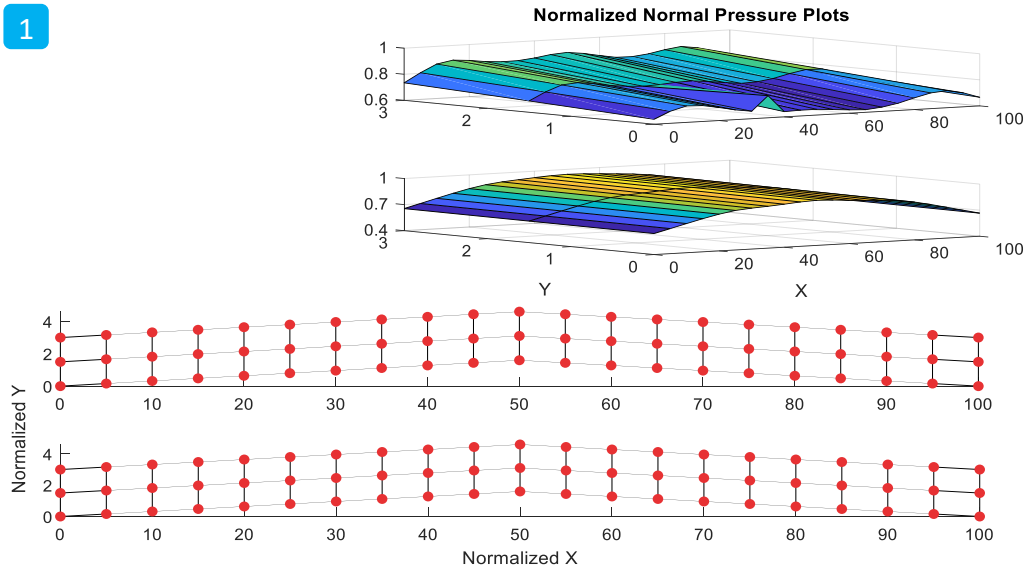

Figure 12: Contact pressure distribution and contact status of the upper and lower contact patch corresponding to the data point 1 of Figure 11

Figure 13: Contact pressure distribution and contact status of the upper and lower contact patch corresponding to the data point 2 of Figure 11

Figure 14: Contact pressure distribution and contact status of the upper and lower contact patch corresponding to the data point 3 of Figure 11
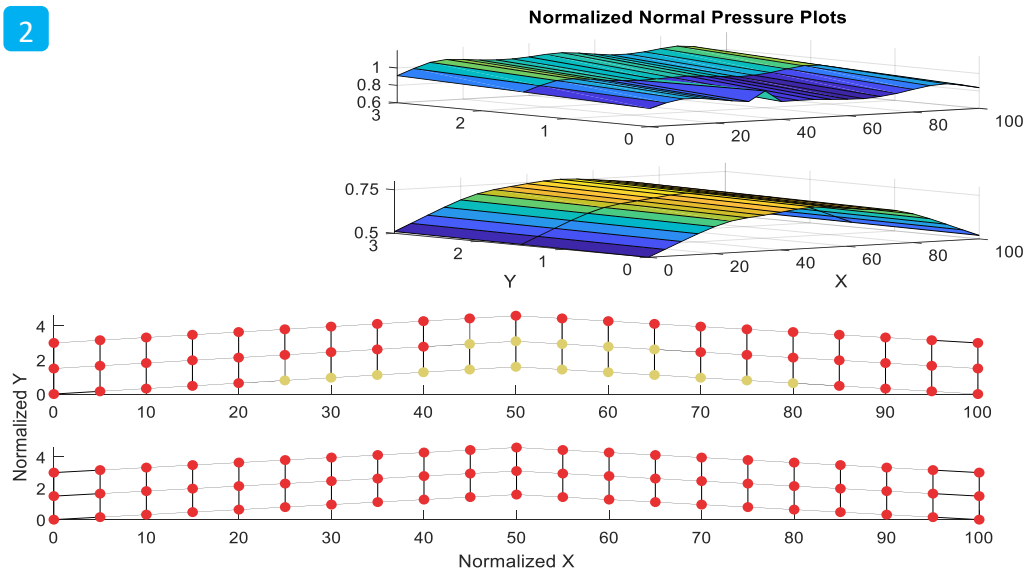

Figure 15: Contact pressure distribution and contact status of the upper and lower contact patch corresponding to the data point 4 of Figure 11

Figure 16: Contact pressure distribution and contact status of the upper and lower contact patch corresponding to the data point 5 of Figure 11
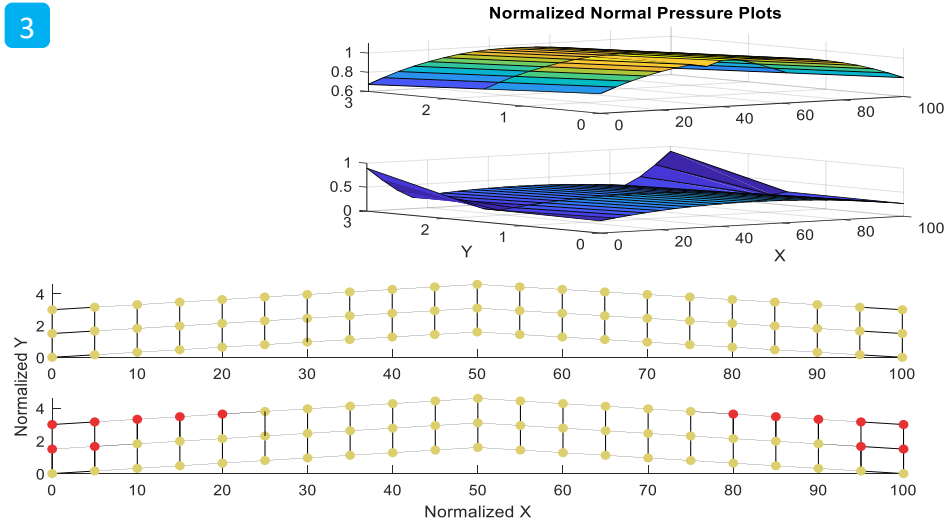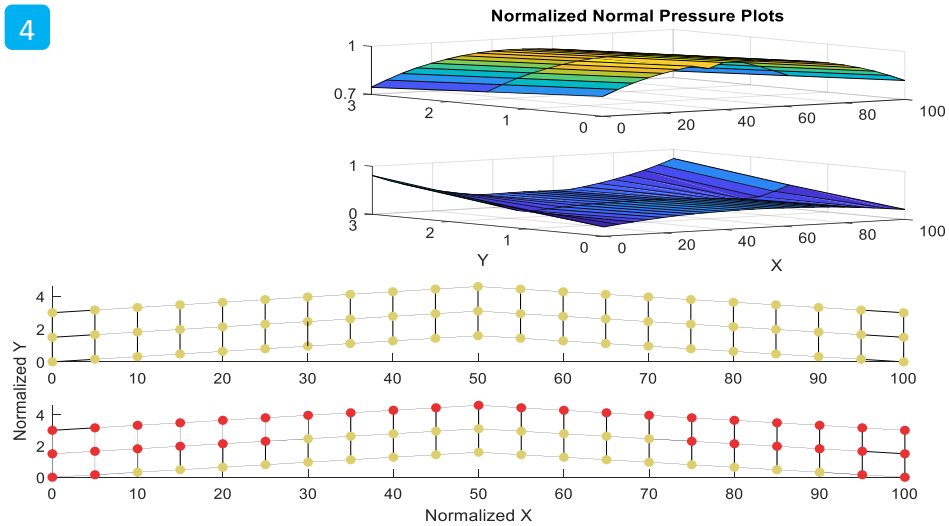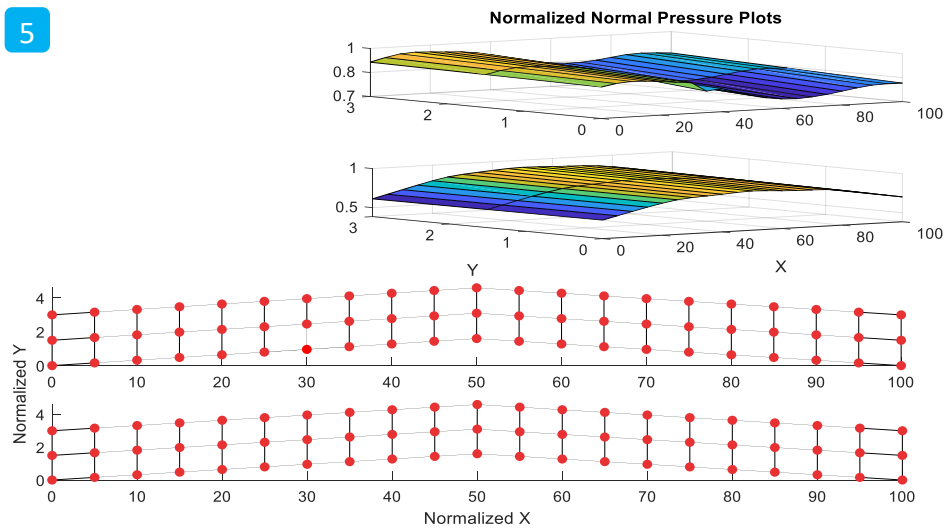
Effect of excitation:

It was interesting to see how the leaf seal responds when subjected to different excitation forces. For all the analyses, the normalized static force was fixed at 3, and the dynamic excitation was varied from 0.1, 0.2, 0.5 and 1. The plots are not shown here due to space constraints. However, the observations are - with low excitation forces, the response tends to follow the linear stick response for the most part with a small softening branch at the resonance like the one showed in the previous section. With increasing excitation force, the peak amplitude and the length of the softening branch increase with increasing the range of nonlinear frequency response giving more chance to have the jump behaviour. Higher excitation forces could cause the premature failure of the leaf seal because of larger separation-stick behaviour of contact nodes at the upper and lower contact patches for wide frequency range.

Effect of normal contact stiffness (K_n):

Similarly, the curiosity of the effect of assumed normal contact stiffness led us to span the numerical experiments on the system. What was seen is, when the system is modelled with higher normal contact stiffness, the overall system tends to get stiffer and vice versa. Because the dynamics of the system in this type of system are highly sensitive to the contact conditions such as contact state and contact stiffness, as this is a numerical investigation at this stage, we make an educated guess of contact stiffness from the prior experience. The usual way to obtain accurate values is through the experiments.

Effect of pin spring stiffness (K_{spring}):

Similarly, it is found that the dynamics of the system are extremely sensitive to the pin spring stiffness values (K_{spring}). In the current system, two soft springs are used to keep the leaf seal in place by resting on the nozzle contact surface in static condition. Hence, the stiffness of these springs plays a major role in governing the dynamics of the leaf. The softer the springs, the dynamic response has high amplitudes and longer softening branches, as the leaf is free to vibrate more than when the springs are stiffer. Hence, the choice of spring is dependent on the trade-off of vibration amplitudes and the required sealing capacity for the operating ranges.

4   Discussion

The nonlinear dynamic analysis is successfully performed on the given combustor leaf seal system and for various operating and kinematic envelopes using the static/dynamic Harmonic Balance Method (HBM) frequency-based method.

The general observations valid for all configurations presented in the results section is as below:

1. The contact elements experience intermittent contact (chattering) along with the upper and lower contact patch at the resonance region. The resonance region is defined here as the frequencies falling under the length of the branch of the softening curve and separating from the linear regime in the dynamic response plots.

2. The 'jump phenomena' with softening behaviour is prevalent in the resonance region for all the operating and kinematic envelopes. However, the length of the softening branch and peak amplitudes are subject to the given configuration.

3. The contact status behaviour and contact pressure plots provide additional information visually, such as the mode shapes in action depending on following the left or the right branch from the resonance region perspective.

4. The response amplitudes outside the resonance region follow the linear stick solution branches, and there is no contact separation (intermittent contact behaviour - chattering).

5. At the extreme configuration of positive inclination of the leaf seal, the contact occurs only at the edges, thereby leaving the centre elements at the contact patch in full separation during a vibration cycle and vice versa for the negative inclination of the leaf seal.

6. For very low excitation forces, the leaf seal response tends towards the 'stick state' response as the static force is three times larger and tries to keep the leaf seal in place. For very high excitation forces, the leaf seal behaves closer to the 'free state' response.

7. The length of the softening response branch and peak response amplitude is qualitative as it depends on the number of factors – frequency range discretization, number of harmonics, pin modelling, etc. With higher harmonics, more accurate resonance amplitudes and length of the softening branch can be obtained, however, at the increased cost of computation.

8. Effect of K_{spring} and K_n on the sensitivity of the results are briefly mentioned. These values greatly affect the dynamic behaviour as the leaf dynamics are highly dependent on the contact conditions.

The computation time taken to obtain the solution for one configuration with a given frequency range is under two minutes with a standard standalone PC. Thanks to the frequency domain solver – HBM. If performing a time-domain analysis to get even the solution at one frequency on the FRF would take hours and sometimes would fail to capture the nonlinear behaviour due to changing contact conditions. The state-of-the-art HBM solver facilitates to model and visualizes complex dynamic behaviour for highly contact nonlinear problems with the underlying assumption of steady-state condition.

5   Conclusions

The current research work successfully presented the nonlinear dynamic analysis performed on the given leaf seal system for various operating and kinematic envelopes using the static/dynamic Harmonic Balance Method (HBM) frequency-based method. The contact is modelled as a unilateral contact in the normal direction to the contact surface. Analysing response plots, it is found that the leaf seal experiences intermittent contact behaviour (chattering) at the resonance region and experiences jump phenomena with softening behaviour causing the leaf to wear at the contact regions and high vibrational amplitudes. In almost all configurations, the leaf seal experience high amplitudes and intermittent contact. These results can be interpreted as a qualitative study to give an overall idea of the complex dynamic behaviour and sensitiveness to the boundary conditions. To validate the numerical results, a test bench is necessary to capture the dynamics experimentally and perform a refined analysis and validation.

Acknowledgements

References

[1] S. Zucca, C. M. Firrone, and M. Gola, "Modeling underplatform dampers for turbine blades: A refined approach in the frequency domain," JVC/Journal Vib. Control, vol. 19, no. 7, pp. 1087–1102, 2013.

[2] L. R. Tamatam, D. Botto, and S. Zucca, "Effect of wear on the dynamics of structures with contact interfaces by a coupled static/dynamic multi-harmonic balance method," in First International Nonlinear Dynamics Conference. Book of abstracts, 2019, no. 1, pp. 129–130.

[3] C. M. Firrone, S. Zucca, and M. M. Gola, "The effect of underplatform dampers on the forced response of bladed disks by a coupled static/dynamic harmonic balance method," Int. J. Non. Linear. Mech., vol. 46, no. 2, pp. 363–375, 2011.

[4] S. Zucca and C. M. Firrone, "Nonlinear dynamics of mechanical systems with friction contacts: Coupled static and dynamic Multi-Harmonic Balance Method and multiple solutions," J. Sound Vib., vol. 333, no. 3, pp. 916–926, 2014.

[5] M. Krack and J. Gross, Harmonic Balance for Nonlinear Vibration Problems. 2019.

[6] G. Jenkins, "Analysis of the stress-strain relationships in reactor grade graphite," Br. J. Appl. Phys., vol. 13, no. 1, pp. 30–32, 1962.

[7] W. D. Iwan, "A Distributed-Element Model for Hysteresis and Its Steady-State Dynamic Response," J. Appl. Mech., vol. 33, no. 4, pp. 893–900, 1966.

[8] C.-H. Menq, J. Bielak, and J. H. Griffin, "The influence of microslip on vibratory response, part I: A new microslip model," J. Sound Vib., vol. 107, no. 2, pp. 279–293, Jun. 1986.

[9] C. C. de Wit, H. Olsson, K. J. Astrom, and P. Lischinsky, "A new model for control of systems with friction," IEEE Trans. Automat. Contr., vol. 40, no. 3, pp. 419–425, 1995.

[10] B. D. Yang and C. H. Menq, "Characterization of 3D Contact Kinematics and Prediction of Resonant Response of Structures Having 3D Frictional Constraint," J. Sound Vib., vol. 217, no. 5, pp. 909–925, 1998.

[11] D. J. Segalman, "A Four-Parameter Iwan Model for Lap-Type Joints," J. Appl. Mech., vol. 72, no. 5, pp. 752–760, 2005.

[12] M. Brake, "A reduced Iwan model that includes pinning for bolted joint mechanics," Nonlinear Dyn., vol. 87, no. 2, pp. 1335–1349, 2017.

[13] R. Bouc, "A Mathematical Model for Hysteresis," Acustica, vol. 24, no. 1, pp. 16–25, 1971.

[14] K. Y. Sanliturk and D. J. Ewins, "Modelling Two-Dimensional Friction Contact and Its Application Using Harmonic Balance Method," J. Sound Vib., vol. 193, no. 2, pp. 511–523, 1996.

[15] E. P. Petrov and D. J. Ewins, "Analytical Formulation of Friction Interface Elements for Analysis of Nonlinear Multi-Harmonic Vibrations of Bladed Disks," J. Turbomach., vol. 125, no. 2, p. 364, 2003.

[16] T. M. Cameron and J. H. Griffin, "An Alternating Frequency / Time Domain Method for Calculating the Steady-State Response of Nonlinear Dynamic Systems," J. Appl. Mech., vol. 56, p. 149, 1989.

[17] O. Poudou and C. Pierre, "Hybrid Frequency-Time Domain Methods for the Analysis of Complex Structural Systems with Dry Friction Damping," 44th AIAA/ASME/ASCE/AHS/ASC Struct. Struct. Dyn. Mater. Conf., no. April, pp. 1–14, 2003.

[18] C. Siewert, L. Panning, J. Wallaschek, and C. Richter, "Multiharmonic Forced Response Analysis of a Turbine Blading Coupled by Nonlinear Contact Forces," J. Eng. Gas Turbines Power, vol. 132, no. 8, p. 082501, 2010.

[19] A. Cardona, A. Lerusse, and M. Géradin, "Fast Fourier nonlinear vibration analysis," Comput. Mech., vol. 22, no. 2, pp. 128–142, 1998.

[20] M. Allara, "A model for the characterization of friction contacts in turbine blades," J. Sound Vib., vol. 320, no. 3, pp. 527–544, 2009.

[21] M. Ciavarella, D. A. Hills, and G. Monno, "The influence of rounded edges on indentation by a flat punch," Proc. Inst. Mech. Eng. Part C J. Mech. Eng. Sci., vol. 212, no. 4, pp. 319–327, 1998.

[22] J. C. Jäger, "A new principle in contact mechanics," ASME J Tribol., vol. 120, no. October 1998, pp. 677–684, 1998.

[23] K. L. Johnson, Contact Mechanics. Cambridge: Cambridge University Press, 1985.

[24] D. Botto and M. Lavella, "A numerical method to solve the normal and tangential contact problem of elastic bodies," Wear, vol. 330–331, pp. 629–635, May 2015.

[25] E. Cigeroglu, N. A. C. H. An, and C. H. Menq, "Forced response prediction of constrained and unconstrained structures coupled through frictional contacts," J. Eng. Gas Turbines Power, vol. 131, no. 2, 2009.

[26] D. Botto and M. Lavella, "High temperature tribological study of cobalt-based coatings reinforced with different percentages of alumina," Wear, vol. 318, no. 1–2, pp. 89–97, 2014.